LASER INTERFEROMETER GRAVITATIONAL WAVE OBSERVATORY
-LIGO-
CALIFORNIA INSTITUTE OF TECHNOLOGY
MASSACHUSETTS INSTITUTE OF TECHNOLOGY

Technical Note **LIGO-T030215- 00- D** July, 2003

Angular Correlation of LIGO Hanford and Livingston Interferometers

M. Rakhmanov and S. Klimenko

This is an internal working note
of the LIGO Project.

California Institute of Technology
LIGO Project - MS 18-34
Pasadena CA 91125
Phone (626) 395-2129
Fax (626) 304-9834
E-mail: info@ligo.caltech.edu

Massachusetts Institute of Technology
LIGO Project - MS NW17-161
Cambridge, MA 02139
Phone (617) 253-4824
Fax (617) 253-4824
E-mail: info@ligo.mit.edu

WWW: http://www.ligo.caltech.edu/

file /home/malik/docs/T030215.ps

Contents

1 Gravitational-Wave Signal

1.1 Two polarizations

Gravitational waves appear as perturbations of the space-time metric. Assume that in the absence of gravitational waves the space-time is flat. Then the metric is

$$g_{\mu\nu} = \eta_{\mu\nu} + h_{\mu\nu}, \tag{1}$$

where $\eta_{\mu\nu}$ is the Minkowski metric and $h_{\mu\nu}$ is the strain tensor of gravitational waves. In the transverse traceless (TT) coordinates the strain tensor takes the form:

$$h_{\mu\nu} = \begin{pmatrix} 0 & & & \\ & h_+ & h_\times & \\ & h_\times & -h_+ & \\ & & & 0 \end{pmatrix}, \tag{2}$$

where h_+ and $h_\times$ correspond to two different polarizations of the gravitational wave. For most of our analysis time can be regarded as a fixed dimension and no time-dependent coordinate transformations will be necessary. We therefore can safely neglect the time components of the 4-dimensional tensors and consider only their spatial (3-dimensional) parts. In this case, the gravitational wave strain tensor can be represented by a sum of two 3-dimensional matrices:

$$\mathbf{h} = h_+\,\mathbf{m} + h_\times\,\mathbf{n}. \tag{3}$$

where $\mathbf{m}$ is a traceless and $\mathbf{n}$ is a transverse unit tensor

$$\mathbf{m} = \begin{pmatrix} 1 & 0 & 0 \\ 0 & -1 & 0 \\ 0 & 0 & 0 \end{pmatrix}, \qquad \mathbf{n} = \begin{pmatrix} 0 & 1 & 0 \\ 1 & 0 & 0 \\ 0 & 0 & 0 \end{pmatrix}. \tag{4}$$

A laser interferometer defines its own coordinate system so that x and y axes run along the two interferometer arms, and the origin is at the beam-splitter. In general, these coordinates are oriented differently from the TT-coordinates of the gravitational wave introduced above. The two coordinate systems can be related by rotational transformation

$$\mathbf{x}' = \mathbf{R}^T\,\mathbf{x}, \tag{5}$$

where $\mathbf{x}$ are the coordinates associated with the gravitational wave and $\mathbf{x}'$ and are the coordinates associated with the detector.

The rotational transformation induces the transformation of the metric. The strain tensor in the detector frame, $\mathbf{h}'$, can be found from the original tensor $\mathbf{h}$ by means of the induced transformation:

$$\mathbf{h}' = \mathbf{R}^T\mathbf{h}\,\mathbf{R}. \tag{6}$$

This can be easily derived from the fact that the length must be conserved:

$$\mathbf{x}'^T\mathbf{h}'\,\mathbf{x}' = \mathbf{x}^T\mathbf{h}\,\mathbf{x}. \tag{7}$$

A laser interferometer generates signal from the difference between the length of the x and y arms, and therefore is proportional to

$$V = \frac{1}{2}\,\mathrm{Tr}\left\{\mathbf{m}\ \mathbf{h}'\right\}. \tag{8}$$

Such a signal is a sum of two parts each originating from an independent polarization:

$$V = F_+\, h_+ + F_\times\, h_\times. \tag{9}$$

The antenna patterns F_+ and $F_\times$ depend on the orientation of the detector with respect to the source and its polarization axes. In the explicit form they are given by

$$F_+ = \frac{1}{2}\,\mathrm{Tr}\left\{\mathbf{m}\,\mathbf{R}^T\mathbf{m}\,\mathbf{R}\right\}, \tag{10}$$

$$F_\times = \frac{1}{2}\,\mathrm{Tr}\left\{\mathbf{m}\,\mathbf{R}^T\mathbf{n}\,\mathbf{R}\right\}. \tag{11}$$

The normalization factors 2^{-1} ensure that the maximum value for the antenna patterns is equal to 1. The orientation of the detector which corresponds to these maximum values is known as optimal.

1.2 Antenna Patterns

The standard antenna patterns can be obtained by using Euler angles for parametrization of the rotational transformations:

$$\mathbf{R} = \mathbf{R}_z(\psi)\ \mathbf{R}_y(\theta)\ \mathbf{R}_z(\phi). \tag{12}$$

The rotations around the x, y, and z axes are given by

$$\mathbf{R}_x(\phi) = \begin{pmatrix} 1 & 0 & 0 \\ 0 & \cos\phi & \sin\phi \\ 0 & -\sin\phi & \cos\phi \end{pmatrix}, \tag{13}$$

$$\mathbf{R}_y(\theta) = \begin{pmatrix} \cos\theta & 0 & -\sin\theta \\ 0 & 1 & 0 \\ \sin\theta & 0 & \cos\theta \end{pmatrix}, \tag{14}$$

$$\mathbf{R}_z(\psi) = \begin{pmatrix} \cos\psi & \sin\psi & 0 \\ -\sin\psi & \cos\psi & 0 \\ 0 & 0 & 1 \end{pmatrix}. \tag{15}$$

Then the antenna patterns [1, 2] can be found as

$$F_+ = 2^{-1}\ \cos 2\phi\,(1+\cos^2\theta)\ \cos 2\psi - \sin 2\phi\ \cos\theta\ \sin 2\psi, \tag{16}$$

$$F_\times = 2^{-1}\ \cos 2\phi\,(1+\cos^2\theta)\ \sin 2\psi - \sin 2\phi\ \cos\theta\ \cos 2\psi. \tag{17}$$

The graphical representation for these functions can be obtained by setting one of the angles to a fixed value. For example, for $\psi = 0$ the antenna patterns are shown in Fig. 1

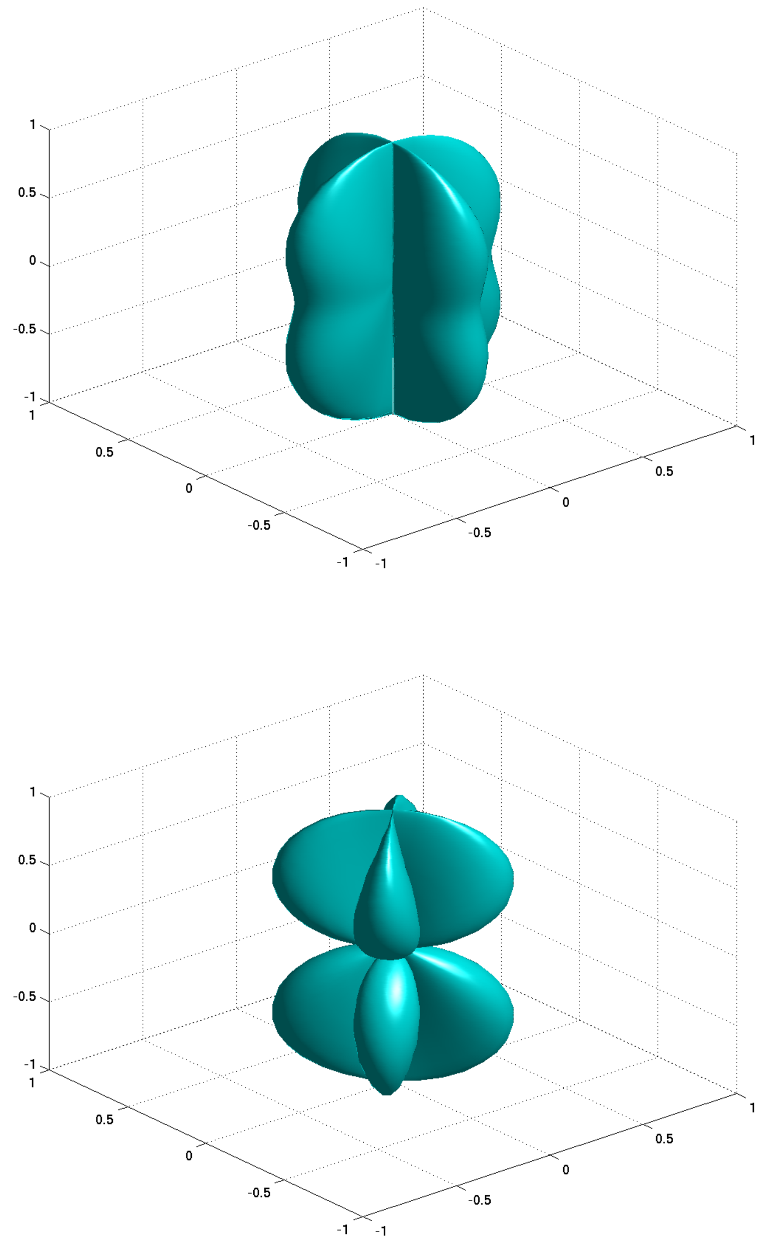

Figure 1: Top: $F_{+}(\phi, \theta, 0)$, bottom: $F_{\times}(\phi, \theta, 0)$.

2 Midpoint Coordinate Frame

All potential sources of gravitational waves are located very far away from the Earth. This fact guarantees that the gravitational waves are well approximated by plane waves

$$h_i(t, \mathbf{x}) = h_i\left(t + \frac{\hat{\mathbf{k}} \cdot \mathbf{x}}{c}\right), \tag{18}$$

where $\hat{\mathbf{k}}$ is a unit vector pointing to the source of the gravitational waves. This representation for the signal indicates that there is a delay in the arrival time of the gravitational wave at the two detector sites. The value for the delay can be found as

$$\tau_s = \frac{\mathbf{k} \cdot \mathbf{p}}{c}, \tag{19}$$

where $\mathbf{p}$ is a vector which originates at one of the detector site and ends at the other, as shown in Fig. 2.

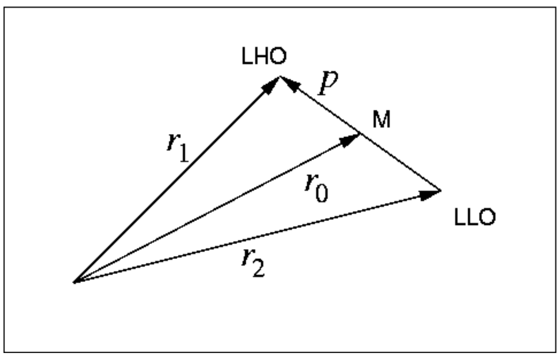

Figure 2: The separation vector and the midpoint for two detectors.

The values of the signal $V(t)$ from each detector depends on the rotational transformation which we parametrize here by some angles. For simplicity, we denote such parametrization by

$$\mathbf{R} = \mathbf{R}(\Omega). \tag{20}$$

These angles may not be independent and may not necessarily form a minimum set. Their choice will be made according to geometrical interpretation and convenience for the analysis.

In order to treat the two detectors as equally as possible, and thus take advantage of symmetry properties of the rotational transformations, we choose the parametrization as follows. We begin by introducing a preferred coordinate system, which is located exactly between the two detectors, as shown in Fig. 2. The advantage of using the midpoint coordinates is that the delay becomes split equally between the two detectors:

$$V_1(t) = F_+(\Omega_1)\, h_+(t + \tau_s/2) + F_\times(\Omega_1)\, h_\times(t + \tau_s/2), \tag{21}$$
$$V_2(t) = F_+(\Omega_2)\, h_+(t - \tau_s/2) + F_\times(\Omega_2)\, h_\times(t - \tau_s/2). \tag{22}$$

The largest delay occurs when the source of gravitational waves is on the line of sight for two detectors (along the vector $\mathbf{p}$):

$$\tau_0 = \frac{|\mathbf{p}|}{c}. \tag{23}$$

This parameter defines a natural time scale in this analysis.

It is important to note that the delay τ_s is not known beforehand unless the location of the source of gravitational waves is known. In general, the analysis strongly depends on whether the location of the source is known or not. The second situation is more difficult and also is more likely to occur in practice.

3 Definition of the Correlation Function

3.1 Correlation Function in Time Domain

Given two signals $V_1(t)$ and $V_2(t)$ which correspond to data streams from two gravitational wave detectors, one can construct the correlation function

$$C(\tau) = \overline{V_1\left(t + \frac{\tau}{2}\right)\ V_2\left(t - \frac{\tau}{2}\right)}. \tag{24}$$

It is a function of the artificial delay: τ. (Note that the artificial delay is introduced in a symmetric manner to be consistent with the midpoint parametrization.) In these notations, maximum correlation, or coincidence, occurs when $\tau = -\tau_s$. Thus defined correlation function is a complicated function of the angular parameters and the time delays:

$$\begin{aligned} C(\tau) \quad = \quad & F_+(\Omega_1)\, F_+(\Omega_2)\ \overline{h_+\left(t + \frac{\tau_s + \tau}{2}\right) h_+\left(t - \frac{\tau_s + \tau}{2}\right)} + \\ & F_+(\Omega_1)\, F_\times(\Omega_2)\ \overline{h_+\left(t + \frac{\tau_s + \tau}{2}\right) h_\times\left(t - \frac{\tau_s + \tau}{2}\right)} + \\ & F_\times(\Omega_1)\, F_+(\Omega_2)\ \overline{h_\times\left(t + \frac{\tau_s + \tau}{2}\right) h_+\left(t - \frac{\tau_s + \tau}{2}\right)} + \\ & F_\times(\Omega_1)\, F_\times(\Omega_2)\ \overline{h_\times\left(t + \frac{\tau_s + \tau}{2}\right) h_\times\left(t - \frac{\tau_s + \tau}{2}\right)}. \end{aligned} \tag{25}$$

However, in reality only the artificial time delay τ is known and therefore we write the correlation function as $C(\tau)$ suppressing all other functional dependences.

It is worthwhile to consider separately these functional dependences and try to gain any information about them. For this purpose we introduce two matrices: $\mathbf{M}$ and $\mathbf{N}$ and write the correlation function in a compact (matrix) form:

$$C(\tau) = \mathrm{Tr}\left\{\mathbf{M}^T\ \mathbf{N}(\tau)\right\}. \tag{26}$$

The first matrix comprises all angular dependence of the correlation function

$$M_{ij} = F_i(\Omega_1)\, F_j(\Omega_2). \tag{27}$$

It does not depend on the delay times or the gravitational wave strain.

The second matrix comprises all temporal behavior of the correlation function

$$N_{ij}(\tau) = \overline{h_i\left(t + \frac{\tau_s + \tau}{2}\right)\, h_j\left(t - \frac{\tau_s + \tau}{2}\right)}. \tag{28}$$

It does not depend on the detector orientations or the location of the source in the sky.

3.2 Correlation Function in Fourier Domain

For computational efficiency, the correlation function is calculated in the Fourier domain. Consider Fourier transformation of the strain function:

$$\tilde{h}_j(\omega) = \int\limits_{-T/2}^{T/2} e^{i\omega t}\, h_j(t)\, dt. \tag{29}$$

Then the Fourier transform of the matrix N_{ij} is

$$\tilde{N}_{ij}(\omega) = e^{i\omega\tau_s}\, \tilde{h}_i(\omega)\, \tilde{h}_j(\omega)^*. \tag{30}$$

As a result, the correlation function takes the form:

$$\tilde{C}(\omega) = \mathrm{Tr}\left\{\mathbf{M}^T\, \tilde{\mathbf{N}}(\omega)\right\}. \tag{31}$$

In practice, the above Fourier transforms are replaced by discrete Fourier transforms defined over the finite time intervals. However, such details are irrelevant for the present analysis.

4 Parametrization of Rotational Transformations

We begin the chain of rotational transformations with the transformation of each detector frame to the midpoint coordinate frame. The two detectors and the center of Earth define the reference plane as shown in Fig. 3. The axes x and z of the midpoint frame are co-planar with the reference plane.

Consider one the detectors, for example, this can be the Hanford detector shown in Fig. 3. The first transformation is such that the x-axis becomes co-planar with the reference plane. This can be achieved by rotating the coordinate frame by angle β_1 around the y-axis. The second transformation is the rotation by $(\pi/2 - \alpha)$ around the y-axis. It will align the detector frame with the midpoint frame. The combined effect of the two transformations is given by the product

$$\mathbf{R}_y(\pi/2 - \alpha)\, \mathbf{R}_z(\beta_1). \tag{32}$$

Similarly, we can construct the transformation from the coordinate frame of the second detector to the midpoint frame. The orientation of the Livingston detector frame with respect to the reference plane involves a different angle: β_2. Furthermore, the second detector is located

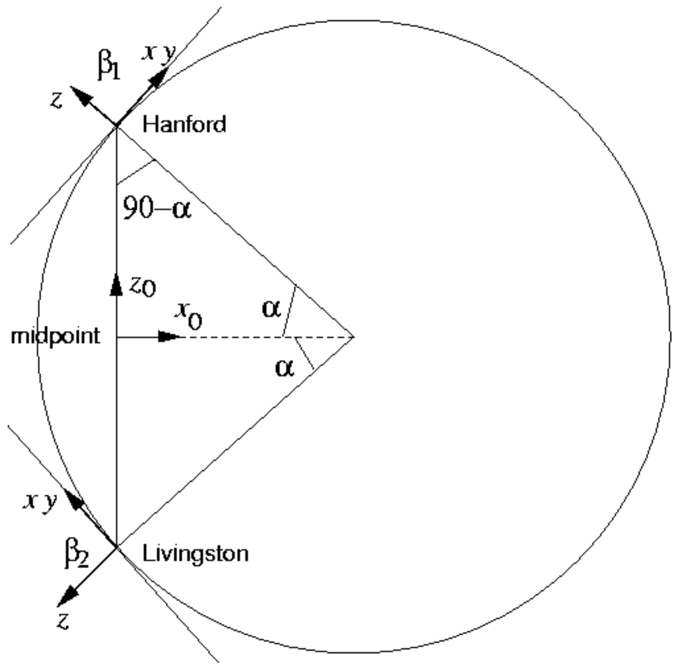

Figure 3: The midpoint and the detector coordinate frames on Earth.

at an angle $-\alpha$ in the reference plane. Therefore, the second rotation angle is $\pi/2 + \alpha$. The combined effect of the two transformations is given by the product

$$\mathbf{R}_y(\pi/2 + \alpha)\ \mathbf{R}_z(\beta_2). \tag{33}$$

The rest of the rotational transformations are the same for both detectors.

We now shall find a coordinate transformation which connects the midpoint frame with the gravitational-wave frame. The midpoint coordinate system, xyz, and the source of gravitational waves, S, are schematically shown in Fig. 4. The location of the source on the sky is given by spherical angles θ and ϕ with respect to the midpoint frame. The third angle, ψ, describes the polarization of the gravitational waves with respect to the plane of incidence (SOP in Fig. 4).

The rotation matrix R_{ij} is defined by the three Euler angles (ϕ, θ, and ψ) and can be constructed as a product of three rotation matrices the same way as in Eq. (12). The only difference is that now the Euler angles are defined in the midpoint frame. It is worthwhile to follow the sequence of the transformations one rotation at a time.

First, we rotate the midpoint frame around the z-axis by the angle ϕ. The axes x and y remain in the horizontal plane. As a result of this transformation, the x-axis comes to point along the direction $\vec{OP}$, which coincides with the projection of $\vec{n}$ onto the plane of the detector. Second, rotate the coordinate frame around the y-axis by the angle θ. As a result of this transformation, the z-axis points to the source ($\vec{OS}$). Also, the axes x and y become perpendicular to $\vec{OS}$.

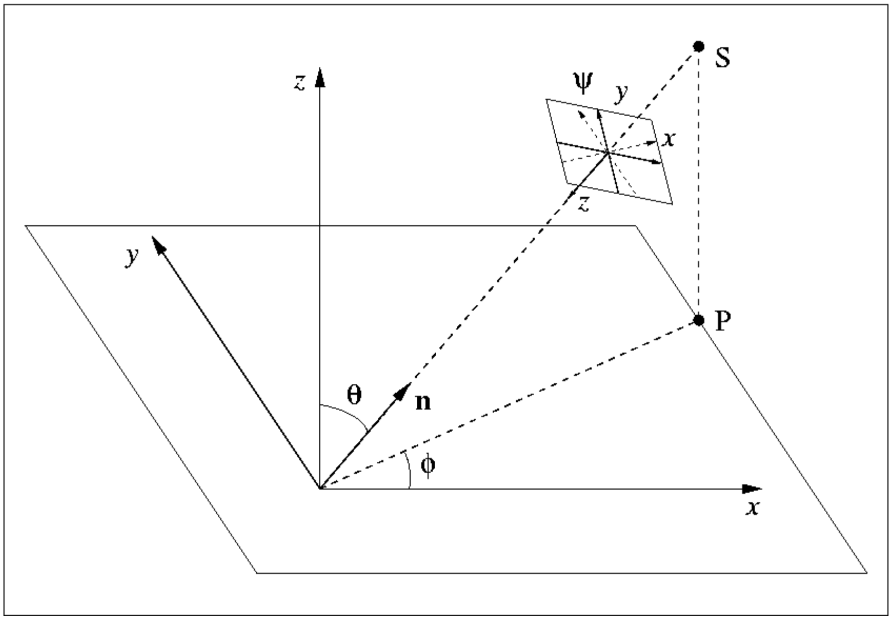

Figure 4: Orientation of the GW coordinate system with respect to the midpoint coordinate system.

Finally, rotate the coordinate frame around the z-axis by the angle ψ. As a result of this transformation, the axes x and y become aligned along the polarization axes of the gravitational wave. The combined effect of all five rotations for the first detector is

$$\mathbf{R}_1 = \mathbf{R}_z(\psi)\ \mathbf{R}_y(\theta)\ \mathbf{R}_z(\phi)\ \mathbf{R}_y(\pi/2-\alpha)\ \mathbf{R}_z(\beta_1). \tag{34}$$

A similar formula can be written for the second detector, except that β_1 must be replaced by β_2 and also α by $-\alpha$:

$$\mathbf{R}_2 = \mathbf{R}_z(\psi)\ \mathbf{R}_y(\theta)\ \mathbf{R}_z(\phi)\ \mathbf{R}_y(\pi/2+\alpha)\ \mathbf{R}_z(\beta_2). \tag{35}$$

In this angular parametrization the delay in the arrival time of the gravitational wave is associated with angle θ. Namely,

$$\cos\theta = \frac{\tau_s}{\tau_0}. \tag{36}$$

Thus all sources which have the same θ coordinate would produce the same delay, regardless of what their ϕ coordinates are.

5 LIGO Hanford and Livingston Detectors

The numerical calculations in this technical note are done for the LIGO Hanford and Livingston 4-km interferometers. The locations of the two detector on Earth are given by their latitudes and longitudes; their orientations are given by the angle between the x-arm and the direction to the North (azimuth) [3, 4].

coordinate	Hanford	Livingston
latitude	$46^0\ 27'\ 18.53''$ N	$30^0\ 33'\ 46.42''$ N
longitude	$119^0\ 24'\ 27.57''$ W	$90^0\ 46'\ 27.27''$ W
azimuth	35.9993^0 N	72.2836^0 S

From these coordinates we conclude that

$$
\begin{aligned}
|\vec{p}| &= 2997.021 \quad \text{km}, && (37)\\
\tau_0 &= 9.996985 \quad \text{ms}, && (38)\\
\alpha &= 13.612^0, && (39)
\end{aligned}
$$

where α is the angle between the z axes of the detectors.

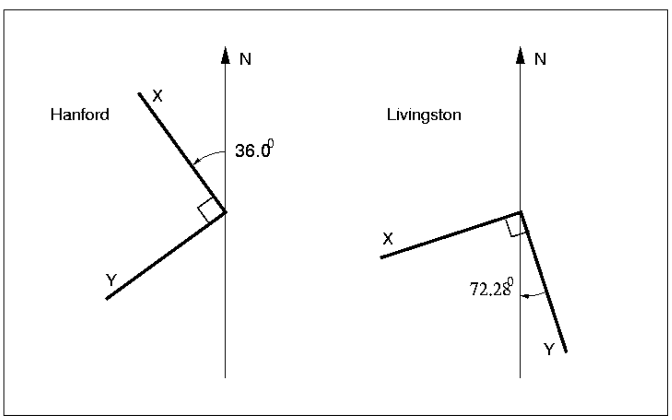

Figure 5: Orientation of the LIGO Hanford and Livingston interferometers in the Earth tangential planes.

Calculations using standard formulas for spherical triangles yield the values for angles β_1 and β_2. These are the angles of x-axis of the detectors and the vector $\vec{p}$:

$$
\begin{aligned}
\beta_1 &= 28.42^0, && (40)\\
\beta_2 &= -61.52^0. && (41)
\end{aligned}
$$

6 Directional Overlap of Two Detectors

The matrix $\mathbf{M}$ depends on the location of the source of gravitational waves on the sky (angles θ and ϕ) and its polarization (angle ψ). In a typical situation neither of these coordinates are known beforehand. Thus, not much can be said about the matrix $\mathbf{M}$. In this situation, one can try guessing the value of the matrix. For example, one can try replacing the matrix $\mathbf{M}$ with its average. There are number of ways we can perform such averaging. Below we describe the results of such averaging in detail.

Average over ψ, ϕ, θ

The simplest would be to average over all three angles. In this case, the angular overlap matrix becomes diagonal:

$$\mathbf{M} = \begin{pmatrix} a & 0 \\ 0 & a \end{pmatrix}, \tag{42}$$

where the coefficient a depends on the mutual detector orientation. For Hanford-Livingston pair numerical analysis yield $a = -0.1413$. The minus sign comes from the fact that the detectors are oriented in such a way that the x arm of one interferometer is roughly parallel to the y arm of another. This form of matrix M is very convenient for calculations but is not particularly useful because it no longer carries the dependence on θ and therefore cannot be used for extracting τ_s.

There is another reason why the diagonal form for matrix M is not useful. It is related to the fact that θ-dependence also occurs in matrix N even though implicitly. Thus consistent averaging over θ would require taking both matrices into account.

Average over ψ, ϕ

The next level of complexity occurs when two of the tree angular degrees of freedom are averaged out. There are three such possibilities. Here we only consider one. In this analysis we are interested in the delay which is related to θ. Therefore, we consider this angle a fixed quantity and average over ψ and ϕ. The result is

$$\mathbf{M}(\theta) = \begin{pmatrix} a(\theta) & b(\theta) \\ -b(\theta) & a(\theta) \end{pmatrix}, \tag{43}$$

where a and b are trigonometric functions of θ. For any two detectors their functional form is

$$a(\theta) = a_0 + a_2 \cos^2\theta + a_4 \cos^4\theta, \tag{44}$$

$$b(\theta) = b_1 \cos\theta + b_3 \cos^3\theta. \tag{45}$$

The coefficients a_i and b_i depend on mutual detector orientation. The relationship between the angle θ and the delay time τ_s, Eq.(36), allows us to express a and b as a function of τ_s. For example, the directional overlap of Hanford-Livingston pair is given by

$$a(\tau_s) = -0.239 + 0.133 \left(\frac{\tau_s}{\tau_0}\right)^2 + 0.084 \left(\frac{\tau_s}{\tau_0}\right)^4, \quad (46)$$

$$b(\tau_s) = 0.073 \left(\frac{\tau_s}{\tau_0}\right) - 0.13 \left(\frac{\tau_s}{\tau_0}\right)^3. \quad (47)$$

This functional dependence is shown in Fig. 6.

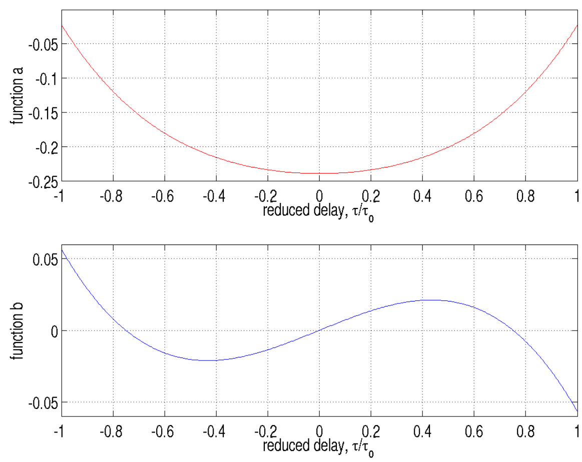

Figure 6: The dependence of the angular parameters a and b on the delay τ_s.

Note that for all values of the delay the coefficient a is negative. This is largely due to the fact that x arm of the Livingston detector is roughly oriented along y arm of the Hanford detector. If we ignore the swap of the arms, the two detectors are aligned as best as possible considering the fact that the detectors belong to the Earth tangential planes at two locations separated by roughly 3000 km. As a result of this alignment the antisymmetric component of the angular correlation b is much less than the symmetric component (roughly a factor of 10 less). The exception is small angle of incidence when the gravitational wave is propagating roughly along vector $\mathbf{p}$. In this case b can be comparable to or greater than a with the maximum value of $b = 2.5718\,a$.

Average over ψ

Finally, one can keep two angular degrees of freedom and average over the third one. Numerical calculations show that the result of such averaging is very complicated. Again, there are three possibilities. Here we only discuss one. Consider a source of gravitational waves with known location on the sky (θ, ϕ) but with unknown polarization (ψ). The matrix $\mathbf{M}$ for such a source can be estimated by taking average over ψ. The result is

$$\mathbf{M}(\theta, \phi) = \begin{pmatrix} a(\theta, \phi) & b(\theta, \phi) \\ -b(\theta, \phi) & a(\theta, \phi) \end{pmatrix}, \quad (48)$$

where a and b are trigonometric functions of both θ and ϕ. For example, for Hanford-Livingston pair these functions are given by

$$
\begin{aligned}
a \quad = \quad & -0.02168 - 0.1909\cos^2\theta + 0.1905\cos^4\theta \\
& -0.06095\cos^4\theta\ \cos^4\phi - 0.1668\cos^4\theta\ \cos^2\phi \\
& -0.06095\cos^4\phi - 0.3423\cdot 10^{-3}\cos\phi\ \sin\phi \\
& +0.5566\cos^2\theta\ \cos^2\phi - 0.3898\cos^2\phi \\
& +0.1219\cos^2\theta\ \cos^4\phi - 0.1731\cos\theta\sin\theta\ \sin\phi \\
& -0.2100\cos^3\theta\sin\theta\ \sin\phi\ \cos^2\phi \\
& -0.1300\cdot 10^{-3}\sin\phi\ \cos^3\phi + 0.3355\cdot 10^{-3}\cos^2\theta\ \cos\phi\ \sin\phi \\
& +0.4323\cos^3\theta\sin\theta\ \sin\phi + 0.2100\cos\theta\sin\theta\ \sin\phi\ \cos^2\phi \\
& -0.1300\cdot 10^{-3}\cos^4\theta\ \cos^3\phi\ \sin\phi \\
& +0.6822\cdot 10^{-5}\cos^4\theta\ \cos\phi\ \sin\phi \\
& +0.2601\cdot 10^{-3}\cos^2\theta\ \cos^3\phi\ \sin\phi,
\end{aligned}
\tag{49}
$$

$$
\begin{aligned}
b \quad = \quad & -0.2064\cos^3\theta - 0.8454\cdot 10^{-4}\cos\phi\ \sin\theta\ \cos^2\theta^2 \\
& +0.09418\sin\phi\sin\theta\ \cos^2\theta + 0.5934\cdot 10^{-3}\cos^2\theta\ \cos^3\phi\ \sin\theta \\
& +0.1965\sin\phi\cos^2\phi\ \sin\theta - 0.3962\cdot 10^{-3}\sin\theta\ \cos\phi \\
& +0.03033\sin\theta\ \sin\phi - 0.5934\cdot 10^{-3}\cos^3\phi\ \sin\theta \\
& +0.1525\cos^3\theta\ \cos^2\phi - 0.1525\cos\theta\cos^2\phi \\
& -0.1965\sin\theta\cos^2\theta\ \sin\phi\cos^2\phi + 0.1496\cos\theta.
\end{aligned}
\tag{50}
$$

There are several ways in which these functions can be analyzed. The simplest is to plot a and b as functions of θ and ϕ. Such a representation is shown in Fig. 7.

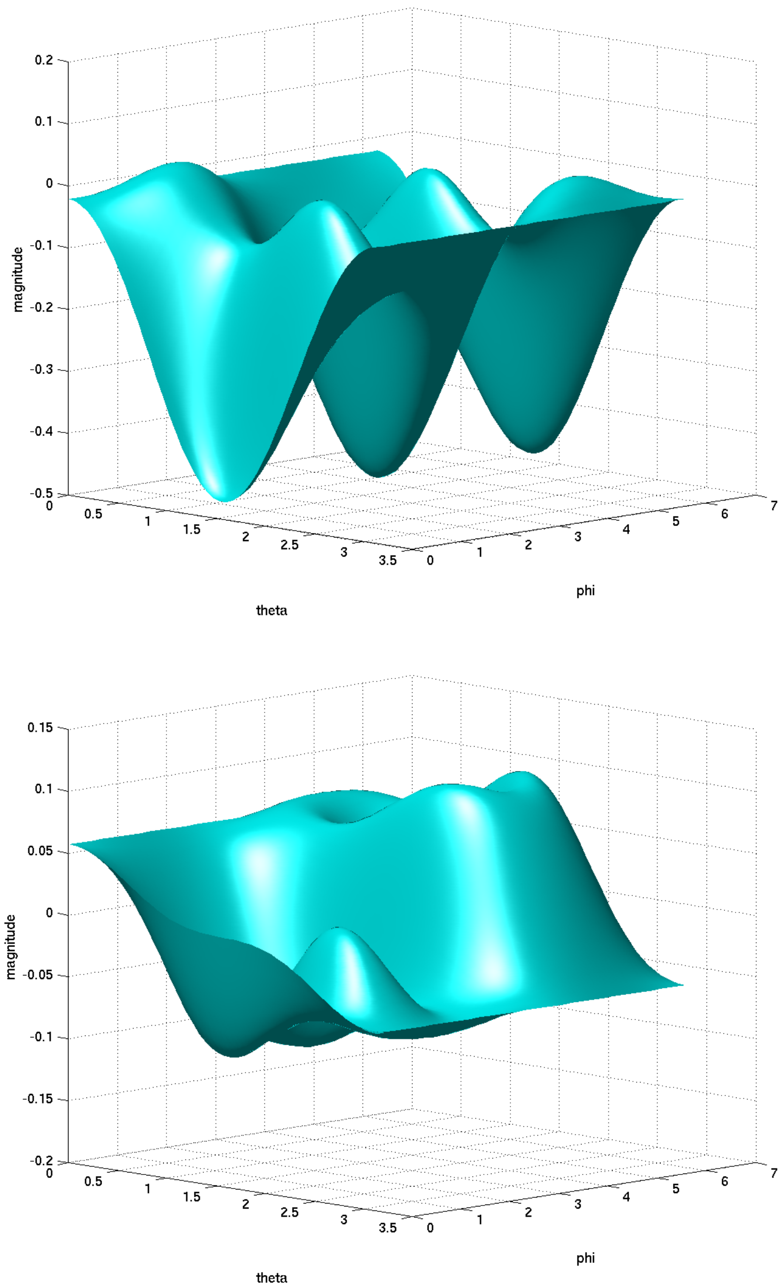

Figure 7: a and b as functions of θ, ϕ.

Another way is to construct a graphical representation similar to the one used to view the standard antenna patterns. In this representation the functions a and b are shown as magnitudes of the radius vector with the spherical angels θ and ϕ. The corresponding Cartesian coordinates are then:

$$x = R \sin\theta \, \cos\phi, \tag{51}$$

$$y = R \sin\theta \, \sin\phi, \tag{52}$$

$$z = R \cos\theta, \tag{53}$$

where R stands either for $|a|$ or $|b|$. Such representation is shown in Fig. 8.

Note that M_{++} (same as a) has a rough cylindrical symmetry along the x-axis. (The x axis of the midpoint coordinate system is directed towards the center of the Earth.) This effect occurs partially because the LIGO Hanford and Livingston interferometers are roughly aligned, and partially because the detector sites are relatively close to each other compared to the size of the Earth. On the other hand, $M_{+\times}$ (same as b) has no obvious symmetry along the x-axis but is roughly symmetric along the y-axis. This fact is rather difficult to explain.

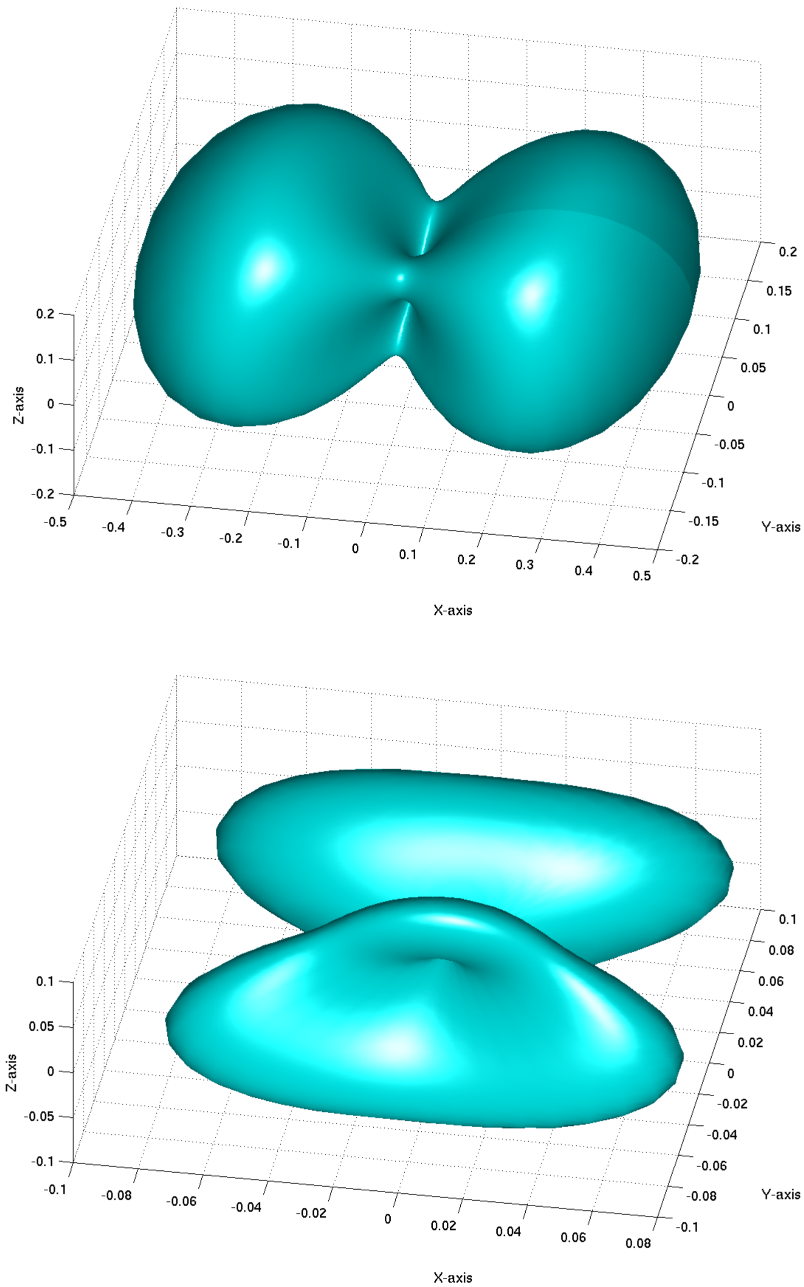

Figure 8: a and b as radius vectors in the Cartesian frame.

Finally, one can analyze the ratio of the two matrix components and form the function:

$$\mu(\theta, \phi) = \frac{b(\theta, \phi)}{a(\theta, \phi)}. \tag{54}$$

This function can be used to find when b-component becomes small compared to a-component. For these angles, one can neglect the b-component making the directional overlap function diagonal. The ratio calculated for the Hanford-Livingston detectors is shown in Fig. 9. The figure can be viewed as a map of the sky showing the regions ("mountains") where the sources of gravitational waves give poor correlation due to strong mixing of the $+$ and x polarizations.

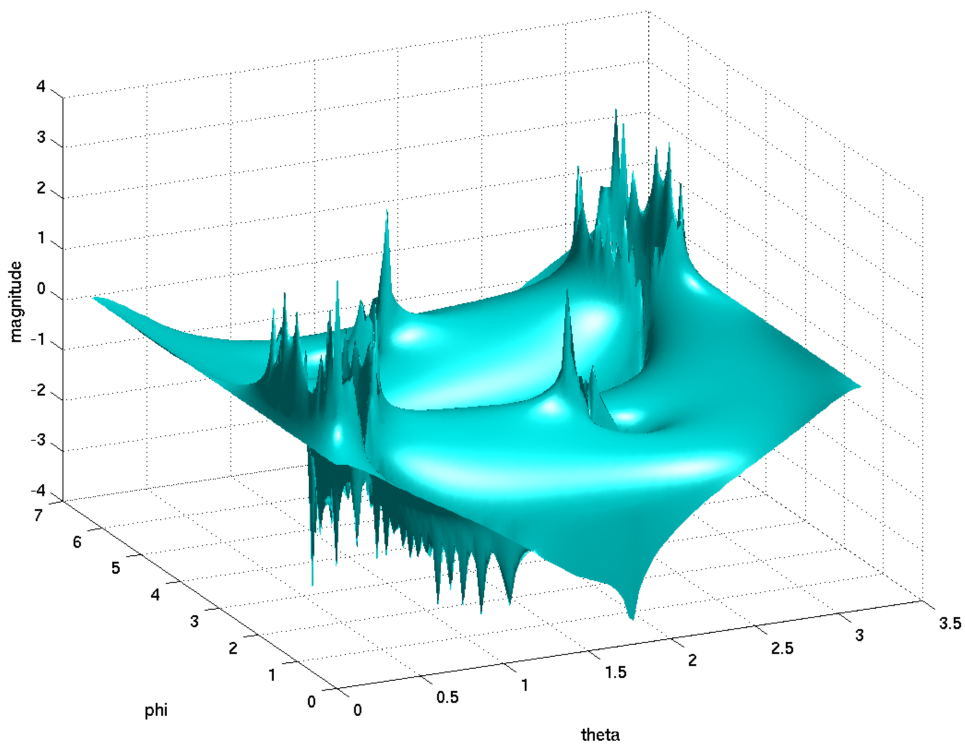

Figure 9: The ration b/a as a function of θ, ϕ.

7 Properties of the Correlation Function

7.1 Real and Imaginary Parts

Assume averaging over ψ and ϕ but not θ. Consider the angular correlation matrix in the form

$$\mathbf{M}(\theta,\phi) = \begin{pmatrix} a(\theta,\phi) & b(\theta,\phi) \\ -b(\theta,\phi) & a(\theta,\phi) \end{pmatrix}. \tag{55}$$

Then the correlation function in time domain becomes

$$\begin{aligned} C(\tau) &= a(\theta,\phi)\left[N_{++}(\tau) + N_{\times\times}(\tau)\right] + &(56)\\ &\quad\; b(\theta,\phi)\left[N_{+\times}(\tau) - N_{\times+}(\tau)\right]. &(57)\end{aligned}$$

Its Fourier-domain representation is

$$\tilde{C}(\omega) = e^{i\omega\tau_s}\left[a\,\mathcal{E}(\omega) + ib\,\mathcal{P}(\omega)\right], \tag{58}$$

where $\mathcal{E}$ is symmetric and $\mathcal{P}$ is antisymmetric function of frequency. The symmetric component is given by

$$\mathcal{E}(\omega) = |\tilde{h}_+(\omega)|^2 + |\tilde{h}_\times(\omega)|^2, \tag{59}$$

and has the meaning of the energy density of the gravitational wave. The antisymmetric component is given by

$$\mathcal{P}(\omega) = \frac{1}{i}\left[\,\tilde{h}_+(\omega)\,\tilde{h}^*_\times(\omega) - \tilde{h}_\times(\omega)\,\tilde{h}^*_+(\omega)\,\right], \tag{60}$$

and has the meaning of the spin density. Both $\mathcal{E}$ and $\mathcal{P}$ are real functions of frequency. (Construction of spin eigenstates for general gravitational wave is given in the Appendix.)

7.2 Magnitude and Phase

For any gravitational wave,

$$|\mathcal{P}(\omega)| \le \mathcal{E}(\omega). \tag{61}$$

The proof of this inequality can be easily done using the helicity eigenstates constructed in the Appendix.

An excess of states with a particular helicity will give rise to nonzero values for the spin density. Such an excess, or imbalance of spin states in the gravitational wave can be characterized by a dimensionless quantity,

$$r(\omega) = \frac{\mathcal{P}(\omega)}{\mathcal{E}(\omega)}, \tag{62}$$

which is bounded by $|r(\omega)| \le 1$. Nonzero values for this quantity would indicate the presence of spin in the gravitational wave and thus confirm the prediction of general relativity.

However, the ratio $r(\omega)$ cannot be directly observed. At best, one can measure the ratio of the detectable spin density to the energy density which is given by

$$r_{\rm obs}(\omega) = \mu(\theta,\phi)\;r(\omega). \tag{63}$$

This relation shows that the ratio $r(\omega)$ becomes suppressed (by a factor of μ) if the detectors are well aligned with respect to each other. Furthermore, for any pair of the detectors even if they are not aligned there are regions of the sky where the source of gravitational wave would not show substantial polarization.

To understand how the ratio $r(\omega)$ can be measured, consider the magnitude and phase of the correlation function:

$$\tilde{C}(\omega) = \mathcal{R}(\omega)\ e^{i\chi(\omega)}. \tag{64}$$

The explicit formula for the magnitude of the correlation function,

$$\mathcal{R}(\omega) = \left[a^2\, \mathcal{E}(\omega)^2 + b^2\, \mathcal{P}(\omega)^2 \right]^{1/2}, \tag{65}$$

shows that the peak value does not necessarily correspond to the maximum of the energy density. Instead, the peak of the magnitude occurs at maximum of the sum of two components in quadrature: $\omega = \omega_p$.

The phase of the correlation function defined as

$$\chi(\omega) = \omega\tau_s + \arctan\left\{ r_{\rm obs}(\omega) \right\}, \tag{66}$$

is directly related to the time delay τ_s. Indeed, the slope of the phase at the peak frequency can be found as

$$\left.\frac{d\chi}{d\omega}\right|_{\omega=\omega_p} = \tau_s + \frac{1}{1 + r^2_{\rm obs}(\omega_p)}\ \left.\frac{dr_{\rm obs}}{d\omega}\right|_{\omega=\omega_p}. \tag{67}$$

Any deviation of the phase from the linear dependence would indicate the presence of the spin density. Thus, the quantity of interest is the difference between the phase of the correlation function and its linear approximation:

$$\delta\chi(\omega) = \chi(\omega) - \left.\frac{d\chi}{d\omega}\right|_{\omega=\omega_p} (\omega - \omega_p). \tag{68}$$

This quantity can be directly measured in the experiment.

A Appendix. Spin-2 Representation of SO(3)

The physical meaning of the symmetric and antisymmetric components of the correlation function can be understood by considering irreducible representations of the rotational group, SO(3). These irreducible representations are specified by spin. Fields that propagate with the speed of light are also characterized by additional quantum number - helicity which is a binary quantity. Due to relativistic constraints helicity can be either $+1$ or -1 depending on whether the spin is oriented along the propagation vector or opposite to it.

For fields propagating with the speed of light, the spin must be oriented parallel to the direction of the wave propagation (z-axis). For gravitational waves, the states with particular helicity are those with spin ↑ or ↓:

$$u(\omega) = \frac{1}{\sqrt{2}}\,[\tilde{h}_+(\omega) + i\tilde{h}_\times(\omega)], \tag{69}$$

$$d(\omega) = \frac{1}{\sqrt{2}}\,[\tilde{h}_+(\omega) - i\tilde{h}_\times(\omega)]. \tag{70}$$

These states are eigenstates of the rotations around the z axis in the TT-coordinate frame. (In this case, the z-axis corresponds to the direction of the wave propagation.)

For these states, rotation by angle α along z-axis generates

$$u(\omega) \to e^{+2i\alpha}\,u(\omega), \tag{71}$$

$$d(\omega) \to e^{-2i\alpha}\,d(\omega). \tag{72}$$

The invariant quantities are the densities of positive and negative helicity:

$$N_\uparrow(\omega) = u(\omega)\,u(\omega)^*, \tag{73}$$

$$N_\downarrow(\omega) = d(\omega)\,d(\omega)^*. \tag{74}$$

Their sum and difference,

$$\mathcal{E}(\omega) = N_\uparrow(\omega) + N_\downarrow(\omega), \tag{75}$$

$$\mathcal{P}(\omega) = N_\uparrow(\omega) - N_\downarrow(\omega), \tag{76}$$

represent the total number of helicity eigenstates and the net spin in the wave. These two quantities are the energy density and the spin density of the gravitational wave.

Some related material can be found in [5, 6, 7, 3, 8, 9].

References

[1] R. Forward, “Wideband laser-interferometer gravitational-radiation experiment,” *Physical Review D*, vol. 17, pp. 379–390, 1978.

[2] K. Thorne, “Gravitational radiation,” in *Three Hundred Years of Gravitation* (S. Hawking and W. Israel, eds.), pp. 330–458, Cambridge University Press, 1987.

[3] W. Althouse, S. Hand, L. Jones, A. Lazzarini, and R. Weiss, “Precision alignment of the ligo 4 km arms using the dual-frequency differential global positioning system,” *Review of Scientific Instruments*, vol. 72, pp. 3086–3094, 2001.

[4] B. Allen, “Gravitational wave detector sites,” technical report, University of Wisconsin – Milwaukee, 2002. arXiv:gr-qc/9607075.

[5] Y. Gürsel and M. Tinto, “Near optimal solution to the inverse problem for gravitational-wave bursts,” *Physical Review D*, vol. 40, pp. 3884–3938, 1989.

[6] B. Schutz, “Data processing, analysis, and storage for interferometric antennas,” in *The Detection of Gravitational Waves* (D. Blair, ed.), Cambridge, England: Cambridge University Press, 1991.

[7] B. F. Schutz and M. Tinto, “Antenna patterns of interferometric detectors of gravitational waves - I. Linearly polarized waves,” *Monthly Notices of the Royal Astronomical Society*, vol. 224, pp. 131–154, 1987.

[8] P. Jaranowski, A. Królak, and B. F. Schutz, “Data analysis of gravitational-wave signals from spinning neutron stars: The signal and its detection,” *Physical Review D*, vol. 58, no. 6, p. 063001, 1998.

[9] S. Bonazzola and E. Gourgoulhon, “Gravitational waves from pulsars: emission by the magnetic-field-induced distortion,” *Astronomy and Astrophysics*, vol. 312, pp. 675–690, 1996.